

Pseudomonas aeruginosa Infection of Zebrafish Involves both Host and Pathogen Determinants[▽]

Anne E. Clatworthy,^{1,2,3} Jenny See-Wai Lee,^{1,2,3} Mark Leibman,^{1,2,3} Zachary Kostun,^{4,5}
Alan J. Davidson,^{4,5} and Deborah T. Hung^{1,2,3,5*}

Department of Molecular Biology and Center for Computational and Integrative Biology, Massachusetts General Hospital, 185 Cambridge St., Boston, Massachusetts 02114¹; Department of Microbiology and Molecular Genetics, Harvard Medical School, Boston, Massachusetts 02115²; Broad Institute of MIT and Harvard, 7 Cambridge Center, Cambridge, Massachusetts 02142³; Center for Regenerative Medicine, Massachusetts General Hospital, 185 Cambridge St., Boston, Massachusetts 02114⁴; and Department of Medicine, Harvard Medical School, Boston, Massachusetts 02114⁵

Received 23 September 2008/Returned for modification 9 November 2008/Accepted 12 January 2009

Zebrafish (*Danio rerio*) have a number of strengths as a host model for infection, including genetic tractability, a vertebrate immune system similar to that of mammals, ease and scale of laboratory handling, which allows analysis with reasonable throughput, and transparency, which facilitates visualization of the infection. With these advantages in mind, we examined whether zebrafish could be used to study *Pseudomonas aeruginosa* pathogenesis and found that infection of zebrafish embryos with live *P. aeruginosa* (PA14 or PAO1) by microinjection results in embryonic death, unlike infection with *Escherichia coli* or heat-killed *P. aeruginosa*, which has no effect. Similar to studies with mice, *P. aeruginosa* mutants deficient in type three secretion (*pscD*) or quorum sensing (*lasR* and *mvfR*) are attenuated in zebrafish embryos infected at 50 h postfertilization (hpf), a developmental stage when both macrophages and neutrophils are present. In contrast, embryos infected at 28 hpf, when only macrophages are initially present, succumb to lethal challenge with far fewer *P. aeruginosa* cells than those required for embryos infected at 50 hpf, are susceptible to infection with *lasR* and *pscD* deletion mutants, and are moderately resistant to infection with an *mvfR* mutant. Finally, we show that we can control the outcome of infection through the use of morpholinos, which allow us to shift immune cell numbers, or small molecules (antibiotics), which rescue embryos from lethal challenge. Thus, zebrafish are a novel host model that is well suited for studying the interactions among individual pathogenic functions of *P. aeruginosa*, the role of individual components of host immune defense, and small-molecule modulators of infection.

Pseudomonas aeruginosa, one of the most common causes of nosocomial infections in the United States, typically infects injured, burned, and immunocompromised patients and is the primary cause of mortality among cystic fibrosis patients. It is a ubiquitous, gram-negative bacterium adapted to a variety of niches, including water and soil in associations with other eukaryotic organisms. A number of evolutionarily divergent model hosts have been used to examine *P. aeruginosa* pathogenesis, including amoebae, plants, nematodes, insects, and rodents (25, 36, 37). While much has been learned about *P. aeruginosa* pathogenesis from these models, each model has different strengths and weaknesses. Invertebrate model hosts such as *Caenorhabditis elegans* offer greater genetic tractability than rodent models. Moreover, the size and life cycle of organisms like *C. elegans* enable experiments such as comprehensive genetic screens that require large numbers of animals, in contrast to rodent models, where such studies are often simply unfeasible due to cost and space requirements. The drawback to modeling human infections in invertebrate hosts is the dissimilarity between vertebrate and invertebrate immune

responses. Invertebrate model hosts such as *Drosophila melanogaster* and *C. elegans* do not possess adaptive immunity, a true complement system, or the immune cell multilineage complexity that is characteristic of humans, although *D. melanogaster* does possess phagocytic cells. Thus, a model host that combines the advantages of invertebrate and rodent models would be extremely powerful in efforts to further understand *P. aeruginosa* pathogenesis.

Zebrafish (*Danio rerio*) have a number of advantages as a model host and thus have been used to study infections with a number of pathogens, including *Mycobacterium marinum*, *Salmonella enterica* serovar Typhimurium, *Edwardsiella tarda*, *Staphylococcus aureus*, and *Streptococcus iniae* (12, 29, 34, 35, 53). Zebrafish are genetically tractable, both forward and reverse classical genetic approaches are possible with this organism (50), and sophisticated techniques using morpholinos and small molecules to precisely control spatiotemporal gene regulation in zebrafish have recently been developed (14, 44). In addition, chemical genetic approaches are feasible; chemical screens for small molecules that modulate a number of phenotypes, including cell cycle progression and nervous and cardiovascular system development, have been performed successfully with zebrafish (33, 47). The capacity to conduct large-scale classical and chemical genetic studies in zebrafish is possible due to their fecundity and small size; embryos/larvae may be kept in a 96-well format during the first 5 to 6 days of development, and a single adult pair of fish can generate ~200

* Corresponding author. Mailing address: Department of Molecular Biology and Center for Computational and Integrative Biology, Massachusetts General Hospital, 185 Cambridge St., Boston, MA 02114. Phone: (617) 643-3117. Fax: (617) 726-6893. E-mail: hung@molbio.mgh.harvard.edu.

[▽] Published ahead of print on 21 January 2009.

embryos from a single mating. Furthermore, zebrafish embryos are optically transparent, which facilitates the visualization of development or infection progression in real time. Finally, zebrafish are jawed vertebrates and thus possess both innate and adaptive immunity similar to that of mammals.

Zebrafish immunity resembles mammalian immunity in a number of ways, including the expression of Toll-like receptors, complement proteins, proinflammatory cytokines, and acute-phase response proteins (5, 10, 23, 26). On a cellular level, zebrafish innate immunity includes a myeloid compartment comprised of both monocyte/macrophage and granulocytic lineages (3). Primitive macrophages have been shown to be capable of engulfing invading microorganisms inoculated at 28 to 30 h postfertilization (hpf) (17, 53), while primitive neutrophil differentiation lags slightly behind, with functional neutrophils appearing by 32 to 48 hpf (22, 34). In contrast, while T-cell progenitors do begin to populate the thymus by 3 days postfertilization, functional maturity of lymphoid cells of the adaptive immune response has not been noted prior to 4 to 6 weeks postfertilization (50).

P. aeruginosa utilizes a number of different virulence mechanisms to combat host defense, including a type three secretion system (T3SS) and the production of multiple exotoxins, including elastase, exotoxin A, and phospholipase C (8, 54). A number of evolutionarily divergent host species, including *Dicystostelium discoideum*, *Arabidopsis thaliana*, *C. elegans*, *D. melanogaster*, *Galleria mellonella*, and rodents, have been used to identify and define the role of these virulence determinants in *P. aeruginosa* pathogenesis (15, 25, 27, 36, 37). Remarkably, these studies have demonstrated that a number of virulence determinants are required for infection across these evolutionarily divergent host species. For example, MvfR, a transcriptional regulator of quorum sensing and virulence, was originally isolated and characterized by using lettuce leaf and *Arabidopsis thaliana* host models (9, 38), but it is also required in *C. elegans* and mouse burn models of *P. aeruginosa* infection (38, 48). Likewise, the quorum-sensing transcriptional regulator LasR, involved in the expression of virulence factors, including elastase, phospholipase C, and exotoxin A, is required for full virulence in both murine (32, 42) and *C. elegans* (49) models. In contrast, the T3SS plays an important role in rodent and insect models (18, 27, 46) but not in *A. thaliana* and *C. elegans* host models (27). Thus, a model host that recapitulates the features of the mammalian (and ideally human) response to *P. aeruginosa* infection yet possesses advantages offered by invertebrate models would be invaluable.

Given the similarities between the zebrafish and mammalian immune responses and the advantages offered by zebrafish as a model organism, we investigated whether we could establish a *P. aeruginosa* infection model in zebrafish embryos. Here we demonstrate that the introduction of *P. aeruginosa* into the circulation of zebrafish embryos establishes a lethal infection that requires quorum sensing and the T3SS for full virulence in late-stage embryos. We have found that ciprofloxacin and imipenem can rescue embryos from lethal challenge. Finally, we examine the contributions of both host and pathogen determinants important for the progression to lethality and place these observations in the context of other *P. aeruginosa* infection models.

MATERIALS AND METHODS

Infection conditions. Zebrafish embryos derived from adults of the AB line were kept at 29°C and staged at 28 hpf (or 50 hpf) according to previously described developmental criteria (19). Embryos were dechorionated manually or with pronase and then anesthetized with 0.015% ethyl 3-aminobenzoate methanesulfonate prior to injection. Bacterial cells (in a volume of 1 or 2 nl) were microinjected into the yolk circulation valley, as visually ascertained under a stereomicroscope. The inoculum size was determined by injecting an equal volume of bacterial cells into phosphate-buffered saline (PBS) in duplicate before and after injections for each needle and enumerating CFU on LB agar; the inoculum size stated throughout is the mean number of cells determined from these dilutions, with the standard deviation, on average, being ~15% of the inoculum size. Injected embryos were returned to embryo medium (E3) (30), incubated at 29°C, and monitored for survival at regular intervals under a stereomicroscope. Very small numbers of bacteria (<140 cells/ml), which had likely leaked from the micropipette during injection and been transferred along with the embryo, were determined to be present in the E3 medium during monitoring. The scoring of living versus dead embryos was ascertained by the presence of a heartbeat and circulating blood under a stereomicroscope. For antibiotic experiments, embryos were placed directly into E3, with or without ciprofloxacin and/or imipenem, following infection by microinjection. All zebrafish experiments were performed with the approval of Massachusetts General Hospital's Institutional Animal Care and Use Committee.

Imaging infection. Microscopy was performed with either a Zeiss Discovery.V12 stereomicroscope (see Fig. 2) or a Zeiss Axio Imager.Z1 microscope equipped with differential interference contrast (DIC) and fluorescence optics, using a $\times 100$ Plan-Apochromat oil immersion objective (numerical aperture = 1.4). Living embryos were anesthetized in E3 medium as described above prior to image acquisition using a stereomicroscope. Living embryos imaged using the Axio Imager.Z1 microscope were anesthetized as described above and mounted on glass depression slides in 1% low-melting-point agarose. Myeloperoxidase activity was detected using fluorescent tyramide (Cy3-TSA amplification reagent; Perkin-Elmer, Waltham, MA) as a substrate for endogenous peroxidase activity, as previously described (34), in embryos that had been fixed in 4% paraformaldehyde overnight at 4°C prior to staining. All images were collected using Axiovision (release 4.5) software.

Bacterial strains and growth conditions. Bacterial cells for microinjection were grown by streaking glycerol stocks on LB-agar plates (with or without antibiotics), incubated overnight at 37°C, and scraped into PBS the following day. The cell concentration was estimated by measuring the optical density at 600 nm of the resulting suspension, which was then diluted to a stock concentration of either 1,250, 2,500, 3,000, 4,000, or 5,000 cells/nl. Cells were passed through a 30-gauge needle 12 times to reduce clumping before loading the cells into a micropipette. The PA14, PA14 $\Delta lasR$, PA14 $\Delta pscD$ (27), and PA14/GFP strains were obtained from Frederick Ausubel (Massachusetts General Hospital). PA14/GFP carries *gfp* on pSMC21 (11). PA14 $\Delta lasR$ has a clean deletion of *lasR* complemented by transforming PA14 $\Delta lasR$ with a plasmid expressing the *lasR* gene in pUCP19 (43). The *pscD* deletion was complemented by allelic exchange using plasmid pEX18 $\Delta pscD1$ (27). The PA14 $\Delta mvfR$ and *mvfR*-complemented strains were obtained from Laurence Rahme (Massachusetts General Hospital) (9), and PAO1 was obtained from Stephen Lory (Harvard Medical School).

Bacterial enumeration from infected embryos. Individual embryos were euthanized with ethyl 3-aminobenzoate methanesulfonate (0.4 mg/ml), washed twice in E3 medium, and disrupted in 0.5 ml E3 medium by use of a 1-ml Dounce homogenizer (0.0035 to 0.0055 in.; Wheaton) for 2 min. Homogenizers were then rinsed with an additional 0.5 ml E3 medium, which was also added to the homogenate. Samples were supplemented with 200 μ l PBS and 130 μ l 1% Triton X-100, vortexed for 1 min prior to bath sonication (Branson 1510 sonicator) for 10 min, and then plated on LB medium supplemented with 15 μ g/ml Irgasan.

Zebrafish morphant generation. The *pu.1* and *gata1* morpholino oligonucleotides, which were described previously (16, 40), were obtained from Gene Tools (Philomath, OR), along with a Gene Tools standard control morpholino. Morpholinos were injected into the embryo at the 1- to 2-cell stage at the following concentrations: *gata1*, 0.2 mM; *pu.1*, 0.4 mM; and standard control, 0.4 mM. Elimination and expansion of the myeloid lineage in Pu.1 and Gata1 morphants, respectively, were confirmed by in situ hybridization to detect L-plastin expression as previously described (16, 40).

SYBR green real-time qRT-PCR analysis. Embryos were infected with PA14, the *lasR* deletion mutant, heat-killed PA14, or *Escherichia coli* DH5 α cells or treated with PBS (sham-infected embryos), and RNAs were isolated from pools of 10 infected and sham-infected homogenized embryos for each condition at each time point, using Trizol reagent (Invitrogen). The resulting RNAs were

used to template first-strand cDNA synthesis reactions, using oligo(dT) and Superscript III reverse transcriptase (both from Invitrogen) according to the manufacturer's instructions. Primers were designed using Primer 3 (41). The sequences of the gene-specific *TNF- α* (GenBank accession no. NM_212859), *IL-1 β* (GenBank accession no. AY340959), and control (*EF1a*) (GenBank accession no. L47669) primers for detection were as follows: *TNF α* F, 5'-TGCTT CACGCTCCATAAGACC-3'; *TNF α* R, 5'-CAAGCCACCTGAAGAAAAGG-3'; *IL1 β* F, 5'-TGGACTTCGCAGCACAAAATG-3'; *IL1 β* R, 5'-CGTTCACCT CACGCTCTTGATG-3'; *EF1a*F, 5'-AGAAGGAAGCCGCTGAGATG-3'; and *EF1a*R, 5'-TGTCCAGGGGCATCAATAAT-3'. One primer from each primer pair overlapped an exon-exon junction. Quantitative reverse transcription-PCRs (qRT-PCRs) were carried out in a total volume of 25 μ l, using cDNA corresponding to 100 ng total RNA and 50 nM gene-specific or control primers. Transcript abundance from each RNA preparation was assayed in triplicate using an ABI 7300 real-time PCR machine (Applied Biosystems). Resulting cycle threshold values from qRT-PCR assays were analyzed by the relative standard curve method and normalized to *EF1a* expression. The changes in *TNF- α* and *IL-1 β* transcript levels relative to those in sham-infected embryos are given as means and standard errors of the means determined for at least three RNA preparations for each experimental condition, which were each assayed in triplicate.

Statistical analysis. Both survival curve and cytokine expression data were graphed and statistically analyzed using GraphPad Prism 4 software. Statistical differences in survival curves were analyzed using the log rank test. Statistically significant differences in tumor necrosis factor alpha (*TNF- α*) and interleukin-1 β (*IL-1 β*) expression between PA14- and either *lasR* mutant-, heat-killed PA14-, or DH5 α -infected embryos were determined for three to five biologic replicates by one-way analysis of variance followed by Bonferroni's multiple comparison test.

RESULTS

Inoculation of embryos with *P. aeruginosa* is lethal. In an effort to develop a *P. aeruginosa* infection model in a genetically tractable vertebrate model host, we investigated whether *P. aeruginosa* could lethally infect zebrafish embryos at 28 hpf, a developmental stage when primitive macrophages are present and able to engulf invading microorganisms postinfection (17, 53). Initial experiments to infect zebrafish with *P. aeruginosa* by immersing dechorionated embryos in a suspension of *P. aeruginosa* strain PA14 failed. Lethality required high concentrations of PA14 (1×10^9 CFU/ml) and was independent of the viability of the bacterial cells (data not shown), suggesting that the toxicity observed was due to a heat-stable component of the bacteria rather than from an active infection. While a lower concentration of *P. aeruginosa* (10^4 CFU/ml) has been shown to colonize the intestinal tract of zebrafish larvae at 3 days postfertilization under similar static immersion conditions (39), we found that this concentration had no effect on embryo viability.

We next explored the possibility of introducing PA14 into the zebrafish embryo bloodstream by microinjection into the yolk circulation valley (Fig. 1A), an area where venous blood returning from the trunk and tail is not contained within a vessel but instead flows freely over the lateral sides of the yolk before returning to the heart. Microinjection at 28 hpf of at least 1,700 PA14 bacterial cells resulted in the death of all infected embryos by ~ 48 h postinfection (hpi) (Fig. 1B), while microinjection of equal or greater numbers of heat-killed PA14 or *Escherichia coli* strain DH5 α resulted in complete survival of infected embryos (Fig. 1B). PA14 killing was dose dependent, with microinjection of fewer than 1,500 cells resulting in incomplete lethality (data not shown). Finally, we examined whether *P. aeruginosa* lethality was specific to the PA14 strain, given that differences in virulence among common *P. aeruginosa* laboratory strains have been observed among different

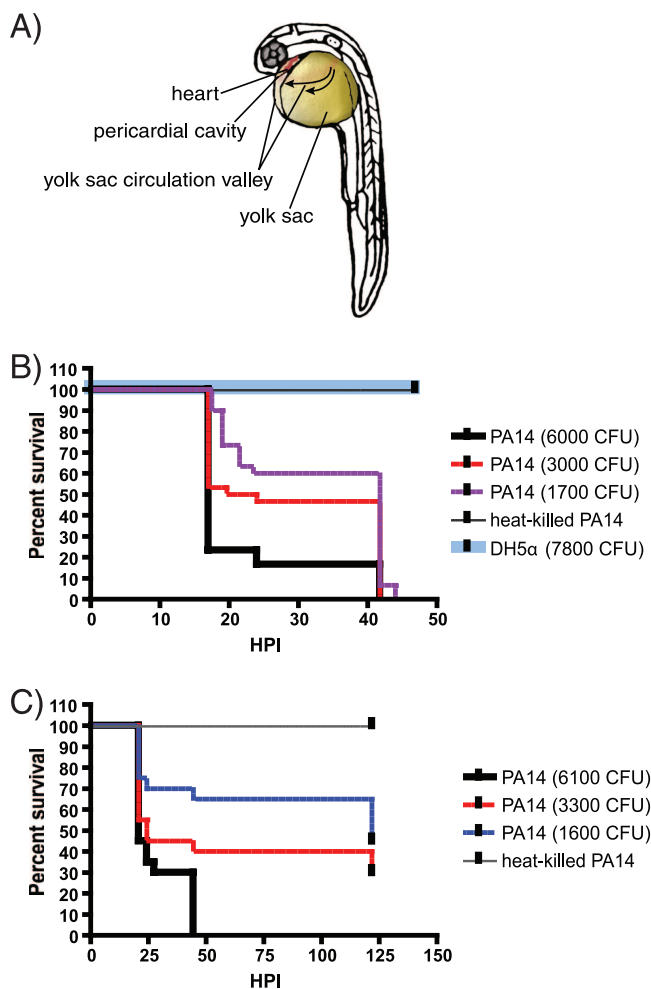


FIG. 1. *P. aeruginosa* infection in zebrafish embryos. (A) Landmarks in the 28 hpf embryo. Arrows indicate the direction of blood flow in the yolk circulation valley. (B) Kaplan-Meier embryo survival curves following infection of 28 hpf embryos with various doses of PA14, heat-killed PA14, or *E. coli* DH5 α . Embryos were monitored for survival at 17 hpi and at regular intervals thereafter. The data are representative of three replicates, with 30 embryos per condition per replicate. (C) Kaplan-Meier embryo survival curves following infection of 50 hpf embryos with various doses of PA14 or heat-killed PA14. Embryos were monitored for survival at 20 hpi and at regular intervals thereafter. The data are representative of three replicates, with 30 embryos per condition per replicate.

model hosts (37, 48), and we found that the PAO1 strain was equally virulent to embryos infected at 28 hpf (data not shown).

We next examined the ability of PA14 to cause lethal infection in zebrafish embryos at a later developmental stage, when both macrophages and neutrophils are present and functional (50 hpf). We found that similar to the case with embryos infected at 28 hpf, microinjection of PA14 into embryos at 50 hpf also elicited a lethal phenotype. However, a higher bacterial dose ($>4,500$ CFU) was required to achieve 100% lethality in embryos infected at 50 hpf (Fig. 1C), suggesting that embryos at 50 hpf are more immunocompetent than those at 28 hpf and can mount a more robust host defense.

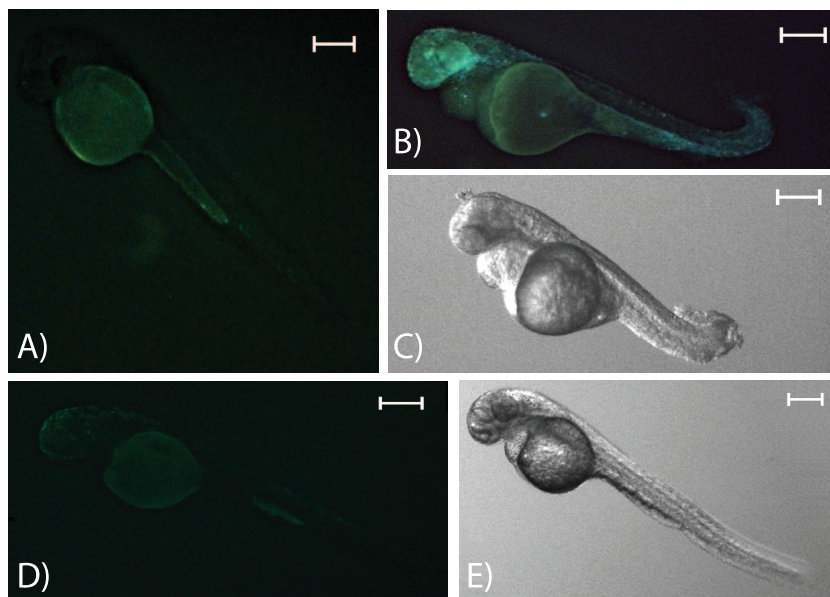


FIG. 2. Visualization of *P. aeruginosa* PA14/GFP infection over time. Embryos staged at 28 hpf were infected with PA14/GFP ($\sim 1,800$ CFU) or heat-killed bacteria and imaged over time. Bars, 200 μ m. (A) Fluorescent image at 4 hpi of an embryo infected with PA14/GFP. (B) Fluorescent image of the embryo in panel A at 22.5 hpi. (C) Bright-field image of the embryo in panel A immediately after death, at 24 hpi. Fluorescent (D) and bright-field (E) images at 22.5 hpi of an embryo infected with heat-killed PA14/GFP are also shown.

Expansion of the bacterial cell population. Zebrafish embryo transparency allowed us to monitor the progression of infection by using PA14 cells expressing green fluorescent protein (PA14/GFP) episomally from a strong constitutive promoter (pSMC21) (11). In the hours immediately following inoculation, GFP fluorescence was undetectable from background autofluorescence throughout the length of the embryo under the magnification offered by a stereomicroscope (Fig. 2A). As infection progressed, the first detectable change observed was a slowing of the embryo circulation and heartbeat, followed by the appearance of GFP fluorescence. At later stages of infection, a few hours prior to death, increasing GFP fluorescence localized to either the area around the eye (Fig. 2B) or the heart and pericardial cavity, with more diffuse GFP fluorescence being detected along the length of the embryo until the time of death (Fig. 2B). Embryo death was often preceded by what appeared to be necrotic cell death in the tail (Fig. 2C). Fluorescence persisted after death for several hours. No fluorescence (above background autofluorescence) was observed in embryos infected with heat-killed PA14/GFP (Fig. 2D).

To gain further insight into the dynamics of PA14 replication during infection of older zebrafish embryos, we examined the overall health, fluorescence pattern, and bacterial load over time in embryos infected at 50 hpf with PA14/GFP. Embryos were infected with PA14/GFP and monitored at 0, 2, 6, 10, 24, and 48 hpi for health and fluorescence. Eight embryos were sacrificed at each time point, homogenized, and plated to examine the bacterial expansion in embryos over time. The inoculum size determined from enumerating bacteria from eight embryos sacrificed immediately following microinjection (10,600 CFU) was similar to the inoculum size determined by plating the injection volume directly from the micropipette (10,200 CFU).

Similar to embryos infected at 28 hpf, the appearance of fluorescence was noted under a stereomicroscope only several hours prior to death and was preceded by a slowing of the embryo heartbeat and a decrease in circulation in the embryo trunk and tail. In order to determine the correlation between the appearance of fluorescence and the bacterial load in each embryo, bacteria were enumerated from four embryos displaying fluorescence (bright) and four embryos that were not fluorescent (dim) at 6 hpi and all subsequent time points; fluorescence was not observed prior to 6 hpi under a stereomicroscope. (Some living, dim embryos were still present at 48 hpi, which is consistent with observed mild variations in time to death, with a mean of 48 h.) In general, GFP fluorescence correlated with a higher bacterial load, with the highest bacterial loads observed reaching 3×10^5 to 4×10^5 cells within 24 hpi (Fig. 3). Conversely, embryos scored as being dim generally had lower bacterial burdens, with a few exceptions. The overlapping bacterial burdens among a few bright and dim embryos may have resulted from both the subjective nature of the analysis and the limited sensitivity of the stereomicroscope in comparing diffuse fluorescence across an entire organism and intense, localized fluorescence. In examining the correlation between bacterial burden and fluorescence, there was partial plasmid loss as the bacteria divided in the absence of selection within the embryo, despite the use of a GFP plasmid that is known to be retained relatively stably in the absence of selection *in vitro* (4). This loss ranged from $\sim 26\%$ at 7 hpi to $\sim 50\%$ at 25 hpi. However, this phenomenon is unlikely to have grossly affected the outcome of the experiment, as the differences in bacterial load between fluorescent and nonfluorescent fish are on the log scale.

Interestingly, the majority of embryos scored as dim between 6 and 48 hpi displayed decreased bacterial burdens compared to the original inoculum. There was variability in the bacterial

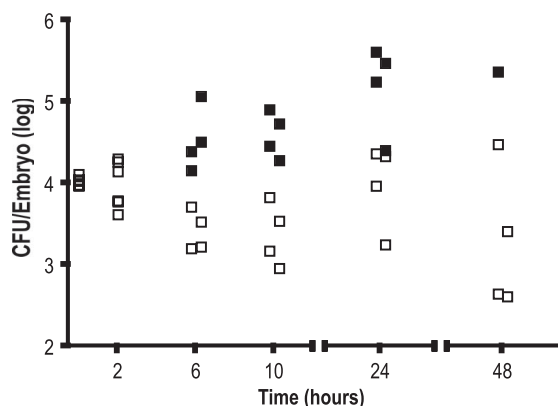


FIG. 3. Expansion of *P. aeruginosa* in embryos over time. Bacterial enumeration from embryos infected at 50 hpf with PA14/GFP (inoculum size, ~10,200 CFU; each point represents CFU recovered from an individual embryo). From 6 to 48 hpi, each embryo was also scored for the presence of fluorescence. ■, fluorescent; □, nonfluorescent.

burden among dim embryos, with about half of them displaying an order of magnitude fewer bacterial cells than the initial inoculum size (Fig. 3). This finding suggests that at least some embryos have the ability to initially control infection and to clear the majority of invading bacteria. At some point, however, this immune control fails, resulting in bacterial expansion and eventually death.

Quorum sensing and the T3SS are required for full virulence only in embryos infected at 50 hpf. To further characterize *P. aeruginosa* infection in zebrafish embryos in the context of other *P. aeruginosa* infection models, we analyzed whether *P. aeruginosa* mutants that are attenuated in other animal models are also attenuated in zebrafish embryos. We examined the ability of PA14 mutants containing in-frame, clean deletions of genes involved in quorum sensing (*lasR*), quorum sensing and the transcriptional regulation of pyocyanin and hydrogen cyanide production (*mvfR*), and the T3SS (*pscD*) to kill embryos infected at 28 and 50 hpf. We found that the survival curves for embryos infected at 28 hpf with wild-type PA14 and either the isogenic *lasR* or *pscD* mutant were not statistically different from one another (Fig. 4A), indicating that the *lasR* and *pscD* mutants are not attenuated in embryos infected at this early developmental stage. However, the survival curve for embryos infected with the *mvfR* mutant was statistically different from the curve generated from embryos infected with wild-type PA14 ($P = 0.01$). Thus, the *mvfR* mutant is moderately attenuated in embryos infected at 28 hpf.

We then infected embryos at 50 hpf with wild-type PA14 and the same panel of deletion mutants to determine whether *P. aeruginosa*'s full virulence arsenal would be required for infection at a later developmental stage, when embryos might be capable of mounting a more robust immune response. In contrast to infection in early-stage embryos, the *lasR* and *pscD* mutants were attenuated in the late-stage embryos (Fig. 4B and D), and the level of attenuation with the *mvfR* mutant was even more pronounced than that in embryos infected at 28 hpf, with 60% survival for embryos infected at 50 hpf (Fig. 4C) and 20% survival

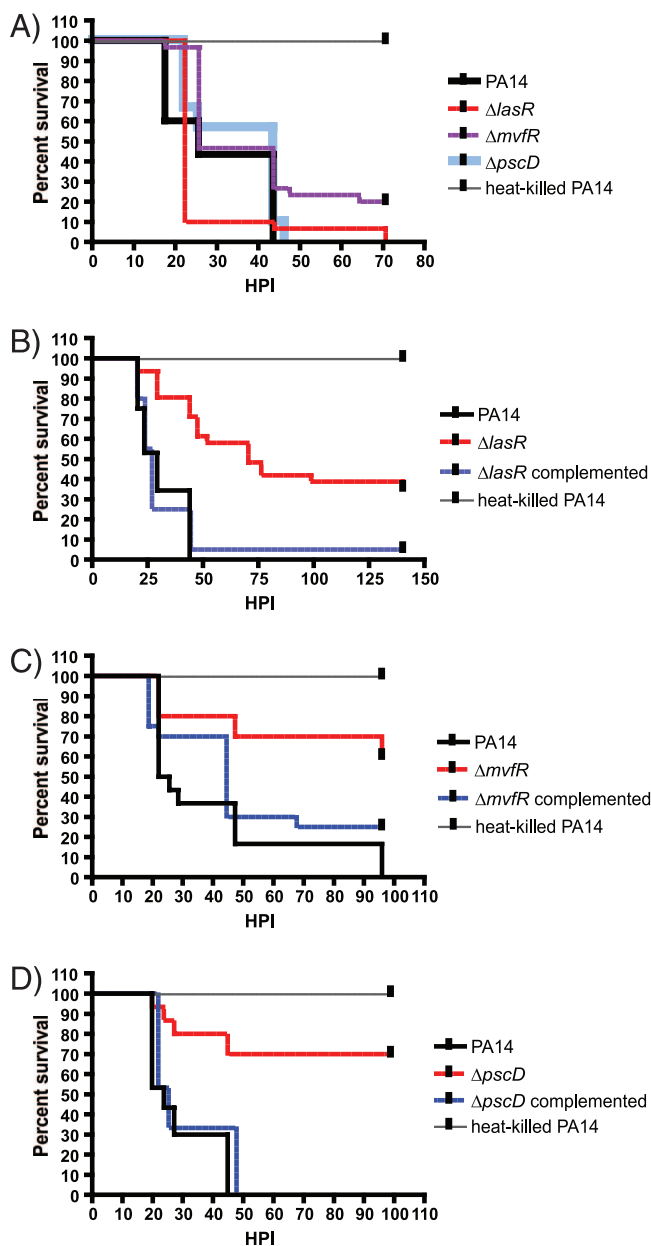


FIG. 4. Susceptibility to quorum sensing and T3SS mutants is dependent on embryo developmental stage. (A) Kaplan-Meier embryo survival curves following infection of 28 hpf embryos with PA14 (~2,300 CFU; $n = 30$), PA14 $\Delta pscD$ (~1,800 CFU; $n = 30$), PA14 $\Delta mvfR$ (~2,400 CFU; $n = 30$), PA14 $\Delta lasR$ (~1,800 CFU; $n = 30$), or heat-killed PA14 ($n = 11$). Embryos were monitored for survival at 17 hpi and at regular intervals thereafter. The data are representative of three replicates. (B) Kaplan-Meier embryo survival curves following infection of 50 hpf embryos with PA14 (~8,000 CFU; $n = 32$), PA14 $\Delta lasR$ (~7,800 CFU; $n = 30$), the PA14 $\Delta lasR$ complemented strain (~6,100 CFU; $n = 20$), or heat-killed PA14 ($n = 12$). (C) Kaplan-Meier embryo survival curves following infection of 50 hpf embryos with PA14 (~6,300 CFU; $n = 30$), PA14 $\Delta mvfR$ (~5,900 CFU; $n = 30$), the PA14 $\Delta mvfR$ complemented strain (~8,100 CFU; $n = 20$), or heat-killed PA14 ($n = 10$). (D) Kaplan-Meier embryo survival curves following infection of 50 hpf embryos with PA14 (~5,000 CFU; $n = 30$), PA14 $\Delta pscD$ (~5,500 CFU; $n = 30$), the PA14 $\Delta pscD$ complemented strain (~6,300 CFU; $n = 30$), or heat-killed PA14 ($n = 5$). Embryos in the experiments for panels B to D were monitored for survival at 20 hpi and at regular intervals thereafter. The data are representative of three replicates.

for embryos infected at 28 hpf with the *mvfR* mutant (Fig. 4A). The survival curves for embryos infected with the deletion mutants at 50 hpf differed significantly from those for embryos infected with the wild-type PA14 strain (P values were <0.0001 in the log rank test between PA14 and each mutant). All mutant phenotypes could be complemented by reintroduction of the respective deleted gene (Fig. 4B to D), with the log rank test between each mutant strain and its corresponding complemented strain giving a P value of <0.05 . Thus, while *lasR*-mediated quorum sensing and the T3SS are not required for full virulence in the infection of early-stage embryos, they are required for full virulence during infection of late-stage embryos. Likewise, the *mvfR* gene is also required for full virulence in late-stage embryos, but it additionally contributes to some degree to virulence during infection of early-stage embryos. While *mvfR* and *lasR* are both involved in regulating quorum-sensing-controlled genes, the genes they positively regulate only partially overlap (13), and *mvfR* has been reported to be a stronger determinant of virulence than *lasR*. Survival has been recorded to be slightly greater for mice infected with *mvfR* mutants than for those infected with the *lasR* mutant (9, 38, 49). Thus, it is not entirely surprising that there is a difference in phenotype between the *lasR* and *mvfR* mutants in embryos infected at 28 hpf, even though they are both generally involved in the transcriptional regulation of genes involved in quorum sensing.

The myeloid cell lineage affects susceptibility to lethal infection. Since the susceptibility to infection with various PA14 mutant strains was dependent on embryo age and thus correlated with the development and function of the host immune defense, we sought to characterize the embryonic immune response to PA14 by examining the contribution of embryonic myeloid cells (macrophages and neutrophils) to defense against *P. aeruginosa* infection. Taking advantage of zebrafish embryo transparency, we were able to visually confirm that PA14/GFP bacteria were indeed engulfed by both myeloperoxidase-positive neutrophils and macrophages (Fig. 5).

We further examined the contribution of myeloid cells to defense against *P. aeruginosa* infection genetically, using morpholino knockdown of transcription factors that regulate myelo- and erythropoiesis. In zebrafish embryos, primitive myeloid and erythroid cells arise from a common myeloid-erythroid progenitor (40), whose fate is determined by the transcription factors Pu.1 and Gata1, which negatively regulate erythroid and myeloid development, respectively (16, 40). Knockdown of Pu.1 shifts progenitor cells to an erythroid cell fate, thus eliminating myeloid cells from the developing embryo and increasing the number of erythroid cells present (40). Gata1 inhibition antithetically commits progenitor cells to a myeloid cell fate, thereby effectively increasing the number of myeloid cells available to combat infection and eliminating erythroid cells (16, 40).

We first confirmed the elimination and expansion of the myeloid lineage in Pu.1 and Gata1 morphants, respectively, by in situ hybridization to detect L-plastin expression (Fig. 6A). We found that Pu.1 morphants were exquisitely susceptible to infection with both wild-type PA14 and the *pscD* mutant in embryos at 50 hpf, confirming that myeloid cells in the devel-

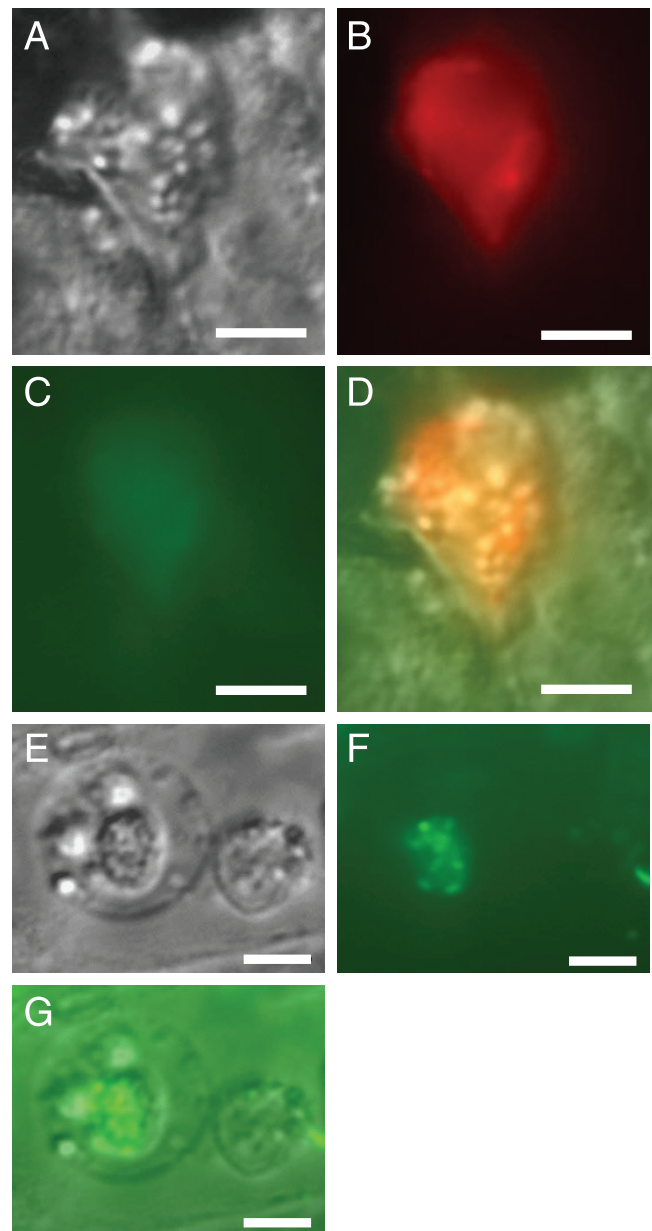


FIG. 5. *P. aeruginosa* colocalizes with myeloid cells. (A to D) DIC (A), Cy3-TSA (B), GFP fluorescence (C), and merged (D) images of a neutrophil from an embryo inoculated at 50 hpf with $\sim 4,300$ PA14/GFP bacterial cells, fixed at 1 hpi, and stained for myeloperoxidase activity with Cy3-TSA. (E to G) DIC (E), GFP fluorescence (F), and merged (G) images of a macrophage obtained from a living embryo inoculated at 50 hpf with $\sim 8,500$ CFU PA14/GFP, captured at 3.75 hpi. Bars, 5 μ m.

oping embryo are required to combat *P. aeruginosa* infection (Fig. 6B). We then determined whether susceptibility to infection with PA14 or the *pscD* mutant could be altered by increasing the number of myeloid cells by Gata1 knockdown. In late-stage embryos (50 hpf), Gata1 morphants were less susceptible to infection with PA14 than control embryos were (Fig. 6C) (for the log rank test between control and Gata1 morphants infected with PA14, $P = 0.0002$), suggesting that the additional numbers of myeloid cells (macrophages and neutrophils)

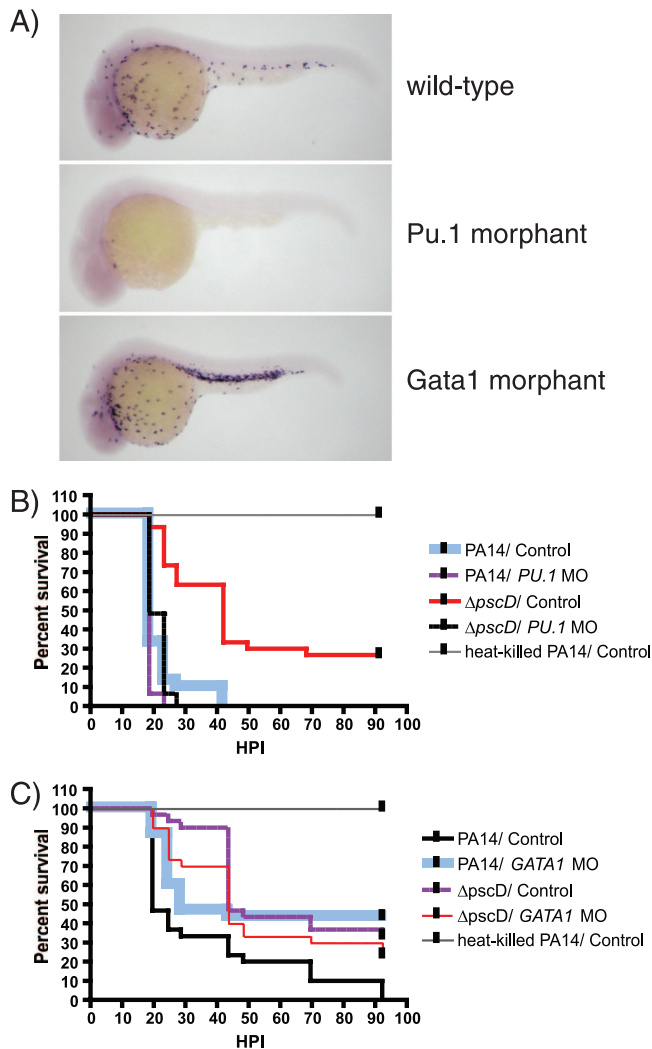


FIG. 6. Myeloid lineage cells control *P. aeruginosa* infection. (A) In situ hybridization to detect L-plastin, a marker for myeloid cells (21), in 24 hpf wild-type (top), Pu.1 (middle), and Gata1 (bottom) morphants. (B) Kaplan-Meier embryo survival curves following inoculation of 50 hpf Pu.1 morphants (PA14, ~5,500 CFU; $\Delta pscD$ strain, ~6,000 CFU) or control morphants (PA14, ~7,000 CFU; $\Delta pscD$ strain, ~5,000 CFU). (C) Kaplan-Meier embryo survival curves following inoculation of 50 hpf Gata1 morphants (PA14, ~6,000 CFU; $\Delta pscD$ strain, ~5,900 CFU) or control morphants (PA14, ~6,700 CFU; $\Delta pscD$ strains, ~4,500 CFU). The data are representative of three replicates, with 30 embryos per condition per replicate.

present at this stage offered greater protection from the lethality of PA14. Interestingly, there was no difference in the survival of either control or Gata1 morphants infected with the *pscD* mutant, suggesting that there is a mode of death independent of the T3SS that cannot be rescued with greater numbers of myeloid lineage cells.

Cytokine response to infection. Since proinflammatory cytokine expression is an integral part of the vertebrate immune response to infection and a clear advantage of modeling *P. aeruginosa* infection in zebrafish rather than in invertebrate hosts, we examined zebrafish proinflammatory cytokine expression in response to PA14 infection. We quantified relative transcript levels of the proinflammatory cytokines TNF- α and

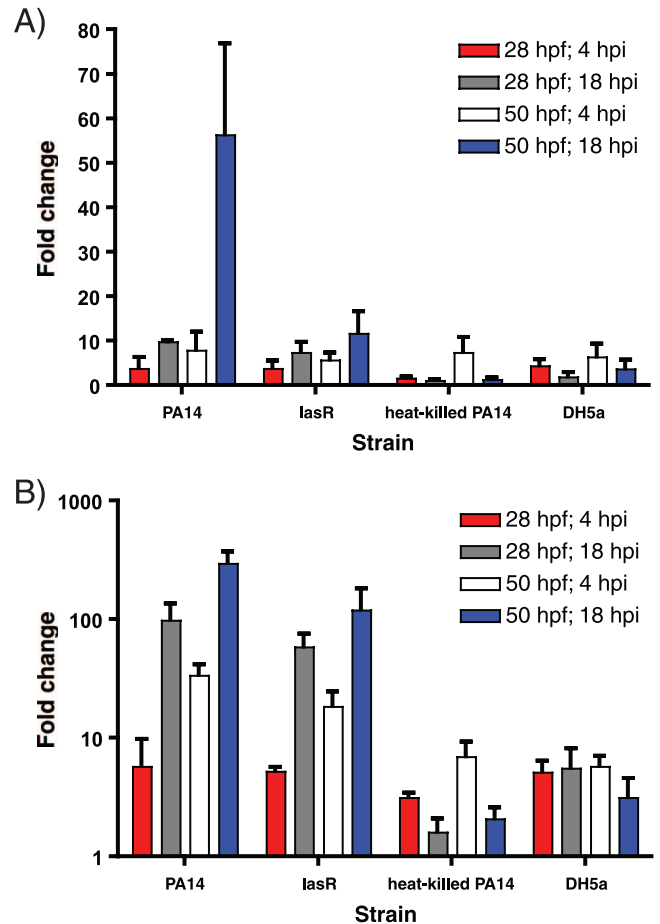


FIG. 7. Proinflammatory cytokine expression following *P. aeruginosa* infection. Relative TNF- α (A) and IL-1 β (B) transcript levels at 4 and 18 hpi were determined by qRT-PCR analysis for embryos that were infected either at 28 hpf with ~2,200 CFU or at 50 hpf with ~7,000 CFU of either PA14, the $\Delta lasR$ strain, heat-killed PA14, or DH5 α cells. Changes in cytokine expression were determined relative to that in sham-infected embryos. Data represent the means and standard errors of the means for at least three biologic replicates.

IL-1 β by real-time RT-PCR for embryos that were infected at 28 or 50 hpf with either PA14, the *lasR* mutant, heat-killed PA14, or *E. coli* DH5 α cells. Embryos that had been infected at 28 hpf demonstrated similar levels of induction of both TNF- α and IL-1 β at 4 hpi, regardless of whether they were infected with PA14, the *lasR* mutant, heat-killed PA14, or DH5 α cells (Fig. 7). By 18 hpi, however, TNF- α and IL-1 β levels in embryos infected with heat-killed PA14 or DH5 α cells had decreased or remained at similar levels compared with levels observed at 4 hpi. In contrast, in embryos infected with live PA14, both TNF- α and IL-1 β transcript levels had increased significantly over the levels observed at 18 hpi in embryos infected with either heat-killed PA14 or DH5 α cells (for TNF- α , $P < 0.01$; for IL-1 β , $P < 0.05$; for the overall data set for TNF- α , $P = 0.0026$; and for the overall data set for IL-1 β , $P = 0.0073$) (Fig. 7).

The proinflammatory cytokine expression pattern observed in embryos infected at 50 hpf with PA14 was even more strik-

ing. While the induction of TNF- α at 4 hpi in embryos infected with PA14 was not statistically different from the level of induction observed with any other strain, the level of TNF- α at 18 hpi in embryos infected with PA14 was statistically significantly higher than levels observed in embryos infected with either heat-killed PA14 ($P < 0.01$) or DH5 α cells ($P < 0.05$) (for the overall data set, $P = 0.0068$) (Fig. 7A). Upregulation of IL-1 β expression was even more dramatic, with expression levels being significantly greater at both 4 hpi ($P < 0.01$; for the overall data set, $P = 0.0058$) and 18 hpi ($P < 0.05$; for the overall data set, $P = 0.0024$) compared to levels in embryos infected with either DH5 α or heat-killed PA14 (Fig. 7B).

In addition to the difference in cytokine responses to PA14, heat-killed PA14, and DH5 α challenge, there was also an interesting difference in cytokine induction between wild-type PA14 and the *lasR* deletion mutant. While there was no statistically significant difference in either TNF- α or IL-1 β expression level at either 4 or 18 hpi in embryos infected at 28 hpf with either PA14 or the *lasR* mutant, there were notable differences in these cytokines in embryos infected at 50 hpf. TNF- α expression at 18 hpi in embryos infected at 50 hpf with the *lasR* deletion mutant was significantly lower ($P < 0.05$; for the overall data set, $P = 0.0068$) than the level observed after infection with PA14 and more closely mirrored the expression level observed following infection with either heat-killed PA14 or DH5 α cells (Fig. 7A). However, there was no statistically significant difference in IL-1 β expression between *lasR* deletion mutant- and wild-type PA14-infected embryos inoculated at 50 hpf (Fig. 7B). Thus, it would appear that levels of TNF- α and not IL-1 β expression late in PA14 infection correlate with death, as the *lasR* mutant is attenuated in embryos infected at 50 hpf.

Small molecules are capable of rescuing embryos from lethal infection. One advantage of using zebrafish embryos to model human disease is the ability to conduct chemical screens for small molecules that perturb a given phenotype in a whole-organism model (24). With this in mind, we examined whether treatment of infected embryos with known antipseudomonad antibiotics could rescue zebrafish embryos from the lethality of PA14 infection. We found that either ciprofloxacin (50 μ g/ml) or imipenem (50 μ g/ml) could rescue 65 to 75% of embryos from lethal *P. aeruginosa* infection when embryos were inoculated at 50 hpf (Fig. 8B). In contrast, embryos infected at 28 hpf required a cocktail of both imipenem (200 μ g/ml) and ciprofloxacin (150 μ g/ml) to rescue similar numbers of embryos (Fig. 8A). It is possible that either the increased immunocompetence of embryos at 50 hpf or potentially an increased ability to absorb antibiotics orally later in infection (as the zebrafish larval mouth opens and intestines become motile at 72 hpf) accounts for the observation that lower concentrations of a single antibiotic can rescue more embryos inoculated at 50 hpf than embryos inoculated at 28 hpf. Notably, the concentrations of antibiotic required for protection are much higher than the MIC of either antibiotic for PA14 in axenic culture (ciprofloxacin MIC = 0.8 μ g/ml; imipenem MIC = 1.6 μ g/ml), suggesting that pharmacokinetic and pharmacodynamic issues of antibiotic distribution in the host dictate the required concentrations for rescue.

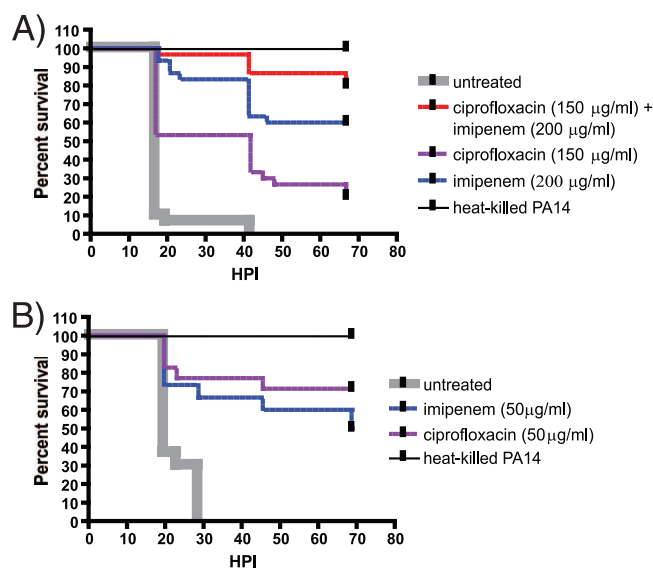


FIG. 8. Antibiotics rescue embryos from lethal infection. (A) Kaplan-Meier embryo survival curves following infection of 28 hpf embryos with PA14 and subsequent immersion in embryo medium containing either ciprofloxacin (150 μ g/ml; $\sim 6,500$ CFU), imipenem (200 μ g/ml; $\sim 6,000$ CFU), a combination of both antibiotics (150 μ g/ml ciprofloxacin and 200 μ g/ml imipenem; $\sim 6,600$ CFU), or no antibiotic ($\sim 6,700$ CFU). Embryos were monitored for survival at 17 hpi and at regular intervals thereafter. The data are representative of three replicates, with 30 embryos per condition per replicate. (B) Kaplan-Meier embryo survival curves following infection of 50 hpf embryos with PA14 and subsequent immersion in embryo medium containing ciprofloxacin (50 μ g/ml; $\sim 8,400$ CFU), imipenem (50 μ g/ml; $\sim 8,500$ CFU), or no antibiotic ($\sim 8,200$ CFU). Embryos were monitored for survival at 19 hpi and at regular intervals thereafter. The data are representative of three replicates, with 30 embryos per condition per replicate.

DISCUSSION

We report that *P. aeruginosa* can establish a lethal infection in zebrafish embryos, thus establishing a new host model for studying *P. aeruginosa* pathogenesis that combines genetic tractability and vertebrate immunity. The outcome of infection can be influenced on the pathogen side by both the inoculum size and the presence of known virulence determinants (*lasR*, *mvfR*, and *pseD*) and on the host side by developmental stage and the presence of immune cells. The outcome of infection can also be modulated by the addition of small molecules to the embryo medium. Using this model, one can examine the complex host-pathogen relationship while manipulating the pathogen and/or the host, using classical or chemical genetics.

Notably, we found that the host response to infection is dependent upon the developmental stage of the embryo. We found that more bacterial cells are required to achieve 100% lethality in embryos inoculated at 50 hpf than in embryos inoculated at 28 hpf. While 28 hpf embryos are slightly shorter in length (~ 2.5 mm) than 50 hpf embryos (~ 3.1 mm), the difference in body mass between 28 and 50 hpf embryos is relatively small and is unlikely to account for the difference in *P. aeruginosa* lethal dose between these two developmental stages. If the toxicity of *P. aeruginosa* at 28 and 50 hpf was related solely to body mass, one would expect the patterns of

susceptibility to infection with the *lasR*, *pscD*, and *mvfR* mutant strains examined to be the same between 28 and 50 hpf embryos. Instead, we found that embryos inoculated at 28 hpf are equally susceptible to infection with either the wild-type PA14 strain or the *lasR* and *pscD* mutant strains, unlike embryos inoculated at 50 hpf. The difference in susceptibility to mutant strains suggests that *P. aeruginosa* requires its full virulence arsenal in 50 hpf embryos in order to create a niche where it can survive and divide. In contrast, *P. aeruginosa*'s full virulence arsenal is not required to create a niche where it can survive and divide within 28 hpf embryos, suggesting that embryos at 28 hpf are less immunocompetent than embryos at 50 hpf to combat *P. aeruginosa* challenge.

The development of host immunity is a complex process that requires a series of coordinated events, including functional differentiation of immune cells, expansion of immune cell populations, and the expression of other immune functions, such as complement proteins. Formally, any one or a combination of these possibilities may account for the difference in immunocompetence between 28 and 50 hpf embryos. Clearly, the presence of myeloid lineage cells is an important step for embryo survival following infection, as evidenced by the rapid death of Pu.1 morphants. Moreover, the expansion of the myeloid population renders embryos less susceptible to infection, as evidenced by the Gata1 morphants, suggesting that the decreased susceptibility of the later embryos could be due to an increase in myeloid cell numbers. However, the difference in phenotype between the two stages of embryos can also be accounted for by differences in functional maturity of the myeloid cells present, as embryos infected at 28 hpf initially do not have functional neutrophils. Clearly, a more detailed understanding of the timing and development of immunologic competence in zebrafish is required before one could attribute a given immunologic function to the difference in phenotype between these two different embryonic stages.

Both macrophages and neutrophils, which we observed to engulf *P. aeruginosa*, are likely to be important in combating *P. aeruginosa* infection in embryos, as they are in human infection. However, the individual contributions of each cell type in controlling *P. aeruginosa* infection in zebrafish embryos cannot currently be determined genetically, as there is no known gene that one could specifically target that would disrupt either macrophage or neutrophil differentiation. While recent work suggests that zebrafish primitive macrophages are able to phagocytose microbes to a far greater extent than primitive neutrophils (21), the individual contributions of macrophages and neutrophils to defense against *P. aeruginosa* infection await further study.

While embryos inoculated at 50 hpf are more capable of successfully mounting a defense against infection with *P. aeruginosa* strains mutated in different virulence mechanisms, they still succumb to infection with wild-type PA14, even though proinflammatory cytokine expression both early and late in infection is robust. It is possible that the consistently high levels of TNF- α observed during PA14 infection may be detrimental to embryonic survival considering TNF- α 's known effects on vascular permeability in mammals. Intraperitoneal injection of high doses of lipopolysaccharide (LPS) alone in mammals are known to result in high levels of expression of TNF- α that can result in dramatic increases in vascular per-

meability and death (51). While fish are thought to be more resistant to LPS toxicity than rodents or calves (2), zebrafish larvae are clearly sensitive to immersion in high concentrations of LPS and display pathophysiologic features characteristic of LPS intoxication similar to those of mammals (1). In this study, the introduction of LPS, in the form of either heat-killed PA14 or DH5 α cells, into the zebrafish embryo bloodstream did not result in high levels of TNF- α transcripts at 18 hpi and was insufficient to result in lethality. Introduction of intact PA14 bacteria, on the other hand, did result in high levels of TNF- α late in infection, and this observation was correlated with death. Whether high levels of TNF- α induction in PA14 infection contribute to embryonic lethality or are simply a marker of PA14 infection awaits further study.

Comparison to other models. The virulence determinants required for infection of zebrafish embryos at 50 hpf are more similar to those required in rodent models of acute *P. aeruginosa* infection (9, 18, 32, 42, 46, 49) than to those required in invertebrate models such as *C. elegans*. The *lasR* and *mvfR* quorum-sensing mutants are attenuated in zebrafish and the mouse burn model to approximately the same degree, with ~50% survival for *lasR* and *mvfR* mutants in both hosts (38, 49). Here we also found that deletion of *pscD* attenuates infection in 50 hpf embryos, and thus, the T3SS is required for full virulence in zebrafish, similar to burn, neutropenic, and acute pneumonia murine infection models (18, 46, 52) and unlike infection in *C. elegans*, where *pscD* is fully dispensable for infection (27). Since intravenous inoculation of zebrafish embryos elicits an acute, bacteremic infection that most closely resembles the mouse burn model of *P. aeruginosa* infection, based on the levels of attenuation of the mutants examined, this model will perhaps be more useful in modeling the systemic *P. aeruginosa* infections that occur in burned and immunocompromised patients than those in chronically infected patients, where mutations in *lasR* and defects in the T3SS have been noted to appear during the course of persistent infection (20, 45).

Advantageous features of a *P. aeruginosa* infection model in zebrafish. One advantage of the *P. aeruginosa* infection model in zebrafish is the ease with which various pathogen components can be analyzed while varying host components, such as examining different *P. aeruginosa* mutants infected at different developmental stages or examining infection while altering immune cell numbers, using morpholinos to shift myeloid and erythroid cell populations. Another advantage is that zebrafish, unlike most host organisms, are amenable to chemical genetics as well as classical genetics (24). Here we find that the outcome of infection can also be modulated by the addition of small molecules to the embryo medium, and thus this model can also be used to probe *P. aeruginosa* pathogenesis in the intact host by using chemical genetics. We showed that forward chemical genetic screens are feasible in this infection model by rescuing infected embryos with small molecules added to the surrounding water. Lower concentrations of antibiotics were sufficient to rescue embryos infected at 50 hpf than at 28 hpf from death. While we do not know the mechanisms for attaining adequate tissue and bloodstream concentrations of antibiotics, passive diffusion of the antibiotics likely occurs and accounts for the success of other reported chemical genetic screens conducted with zebrafish embryos (33, 47).

Chemical screening of whole-organism infection models is an attractive approach for identifying the next generation of antimicrobials, particularly given the current climate, where antibiotic resistance is outpacing antibiotic discovery and development. Our current antibiotic stockpile is composed largely of variations of compounds discovered ~40 to 60 years ago by their ability to kill or inhibit the growth of logarithmically growing bacterial cells in vitro. Since that time, with the exceptions of the narrow-spectrum drugs daptomycin and linezolid, no new classes of clinically relevant antibiotics have been discovered. More recent efforts using target-based approaches to identify inhibitors of gene products thought to be essential for bacterial viability have largely been unsuccessful (31). Unlike target-based assays, however, whole-organism screening has the potential to directly identify compounds that are effective at eliciting the desired phenotype (such as attenuation of infection) and has the potential to leapfrog over some of the major hurdles associated with drug development in that whole-organism screening inherently selects for compounds that are cell permeable, have little to no gross toxic side effects, and have acceptable pharmacokinetic profiles (at least in the model host) (24). While examples of whole-organism screening for anti-infectives in rodent models are extremely rare due to space, cost, and even ethical considerations, they have historically resulted in the successful discovery of drugs such as ivermectin, an antiparasitic therapeutic (7). Recent efforts to conduct whole-organism screening of invertebrate infection models have overcome many of the drawbacks associated with screening of rodent infection models and have been used successfully to identify compounds effective at attenuating *Enterococcus faecalis* and *Candida albicans* infection in *C. elegans* (6, 28). The drawback to screening whole-organism invertebrate infection models, of course, is the relative dissimilarity between the invertebrate and mammalian immune responses to infection. Since zebrafish are vertebrates with an immune system similar to that of mammals, whole-organism screening of zebrafish infection models may be more effective at identifying compounds useful in treating human infections.

We have demonstrated that zebrafish represent an effective new model for examining *P. aeruginosa* pathogenesis that has many advantages, including ease of manipulating the immune response in the setting of optical transparency. While visualizing and manipulating the immune response in rodent models are technically feasible using intravital microscopy and genetic tools, such studies will be technically easier, faster, and cheaper with zebrafish. Thus, zebrafish as a model host may provide a unique forum in which to conduct comprehensive studies of pathogen mutants in the context of variations in host immunity and to explore individual contributions of macrophage and neutrophil lineages to host defense. Given the ability to conduct both classical and chemical genetic studies, the ability to manipulate host immunity, and the ability to examine the infection as it progresses in the living organism, the zebrafish infection model is a useful complement to and combines the strengths of existing models of *P. aeruginosa* infection.

ACKNOWLEDGMENTS

We thank F. Ausubel, S. Lory, and L. Rahme for strains and plasmids. We also thank L. Ramakrishnan, J. Rawls, and R. Peterson and his lab for helpful discussions, R. Smith and E. Drenkard for critical

readings of the manuscript, and N. Chand and A. Kuchena for technical assistance.

This work was funded by grants from the Broad Institute and the Pew Scholars in Biomedical Sciences Program.

ADDENDUM IN PROOF

Since acceptance of our paper, we acknowledge that M. K. Brannon, J. M. Davis, J. R. Mathias, C. J. Hall, J. C. Emerson, P. S. Crosier, A. Huttenlocher, L. Ramakrishnan, and S. M. Moskowitz (Cell. Microbiol., in press) have also found that *Pseudomonas aeruginosa* infection is lethal to zebrafish embryos and that infection of embryos 50 h postfertilization is dependent upon a functional type III secretion system.

REFERENCES

- Bates, J. M., J. Akerlund, E. Mittge, and K. Guillemin. 2007. Intestinal alkaline phosphatase detoxifies lipopolysaccharide and prevents inflammation in zebrafish in response to gut microbiota. *Cell Host Microbe* 2:371–382.
- Berczi, L., L. Bertok, and T. Bereznoi. 1966. Comparative studies on the toxicity of *Escherichia coli* lipopolysaccharide endotoxin in various animal species. *Can. J. Microbiol.* 12:1070–1071.
- Berman, J. N., J. P. Kanki, and A. T. Look. 2005. Zebrafish as a model for myelopoiesis during embryogenesis. *Exp. Hematol.* 33:997–1006.
- Bloembergen, G. V., G. A. O'Toole, B. J. Lugtenberg, and R. Kolter. 1997. Green fluorescent protein as a marker for *Pseudomonas* spp. *Appl. Environ. Microbiol.* 63:4543–4551.
- Boshra, H., J. Li, and J. O. Sunyer. 2006. Recent advances on the complement system of teleost fish. *Fish Shellfish Immunol.* 20:239–262.
- Breger, J., B. B. Fuchs, G. Aperis, T. I. Moy, F. M. Ausubel, and E. Mylonakis. 2007. Antifungal chemical compounds identified using a *C. elegans* pathogenicity assay. *PLoS Pathog.* 3:168–178.
- Campbell, W. C. 2005. Serendipity and new drugs for infectious disease. *ILAR J.* 46:352–356.
- Cao, H., R. L. Baldini, and L. G. Rahme. 2001. Common mechanisms for pathogens of plants and animals. *Annu. Rev. Phytopathol.* 39:259–284.
- Cao, H., G. Krishnan, B. Goumnerov, J. Tsongalis, R. Tompkins, and L. G. Rahme. 2001. A quorum sensing-associated virulence gene of *Pseudomonas aeruginosa* encodes a LysR-like transcription regulator with a unique self-regulatory mechanism. *Proc. Natl. Acad. Sci. USA* 98:14613–14618.
- Clay, H., J. M. Davis, D. Beery, A. Huttenlocher, S. E. Lyons, and L. Ramakrishnan. 2007. Dichotomous role of the macrophage in early *Mycobacterium marinum* infection of the zebrafish. *Cell Host Microbe* 2:29–39.
- Cowan, S. E., E. Gilbert, A. Khlebnikov, and J. D. Keasling. 2000. Dual labeling with green fluorescent proteins for confocal microscopy. *Appl. Environ. Microbiol.* 66:413–418.
- Davis, J. M., H. Clay, J. L. Lewis, N. Ghorri, P. Herbolmel, and L. Ramakrishnan. 2002. Real-time visualization of mycobacterium-macrophage interactions leading to initiation of granuloma formation in zebrafish embryos. *Immunity* 17:693–702.
- Deziel, E., S. Gopalan, A. P. Tampakaki, F. Lepine, K. E. Padfield, M. Saucier, G. Xiao, and L. G. Rahme. 2005. The contribution of MvIR to *Pseudomonas aeruginosa* pathogenesis and quorum sensing circuitry regulation: multiple quorum sensing-regulated genes are modulated without affecting *lasRI*, *rhlRI* or the production of *N*-acyl-L-homoserine lactones. *Mol. Microbiol.* 55:998–1014.
- Eseoglu, H., V. Chang, J. K. Mich, and J. K. Chen. 2007. Small molecule regulation of zebrafish gene expression. *Nat. Chem. Biol.* 3:154–155.
- Fauvarque, M. O., E. Bergeret, J. Chabert, D. Dacheux, M. Satre, and I. Attree. 2002. Role and activation of type III secretion system genes in *Pseudomonas aeruginosa*-induced *Drosophila* killing. *Microb. Pathog.* 32:287–295.
- Galloway, J. L., R. A. Wingert, C. Thisse, B. Thisse, and L. I. Zon. 2005. Loss of gata1 but not gata2 converts erythropoiesis to myelopoiesis in zebrafish embryos. *Dev. Cell* 8:109–116.
- Herbolmel, P., B. Thisse, and C. Thisse. 1999. Ontogeny and behavior of early macrophages in the zebrafish embryo. *Development* 126:3735–3745.
- Holder, I. A., A. N. Neely, and D. W. Frank. 2001. Type III secretion/intoxication system important in virulence of *Pseudomonas aeruginosa* infections in burns. *Burns* 27:129–130.
- Kimmel, C. B., W. W. Ballard, S. R. Kimmel, B. Ullmann, and T. F. Schilling. 1995. Stages of embryonic development of the zebrafish. *Dev. Dyn.* 203:253–310.
- Lee, V. T., R. S. Smith, B. Tummler, and S. Lory. 2005. Activities of *Pseudomonas aeruginosa* effectors secreted by the type III secretion system in vitro and during infection. *Infect. Immun.* 73:1695–1705.
- Le Guyader, D., M. J. Redd, E. Colucci-Guyon, E. Murayama, K. Kissa, V. Briolat, E. Mordelet, A. Zapata, H. Shinomiya, and P. Herbolmel. 2008. Origins and unconventional behavior of neutrophils in developing zebrafish. *Blood* 111:132–141.

22. Lieschke, G. J., A. C. Oates, M. O. Crowhurst, A. C. Ward, and J. E. Layton. 2001. Morphologic and functional characterization of granulocytes and macrophages in embryonic and adult zebrafish. *Blood* **98**:3087–3096.
23. Lin, B., S. Chen, Z. Cao, Y. Lin, D. Mo, H. Zhang, J. Gu, M. Dong, Z. Liu, and A. Xu. 2007. Acute phase response in zebrafish upon *Aeromonas salmonicida* and *Staphylococcus aureus* infection: striking similarities and obvious differences with mammals. *Mol. Immunol.* **44**:295–301.
24. MacRae, C. A., and R. T. Peterson. 2003. Zebrafish-based small molecule discovery. *Chem. Biol.* **10**:901–908.
25. Mahajan-Miklos, S., L. G. Rahme, and F. M. Ausubel. 2000. Elucidating the molecular mechanisms of bacterial virulence using non-mammalian hosts. *Mol. Microbiol.* **37**:981–988.
26. Meijer, A. H., S. F. Gabby Krens, I. A. Medina Rodriguez, S. He, W. Bitter, B. Ewa Snaar-Jagalska, and H. P. Spaik. 2004. Expression analysis of the Toll-like receptor and TIR domain adaptor families of zebrafish. *Mol. Immunol.* **40**:773–783.
27. Miyata, S., M. Casey, D. W. Frank, F. M. Ausubel, and E. Drenkard. 2003. Use of the *Galleria mellonella* caterpillar as a model host to study the role of the type III secretion system in *Pseudomonas aeruginosa* pathogenesis. *Infect. Immun.* **71**:2404–2413.
28. Moy, T. I., A. R. Ball, Z. Anklesaria, G. Casadei, K. Lewis, and F. M. Ausubel. 2006. Identification of novel antimicrobials using a live-animal infection model. *Proc. Natl. Acad. Sci. USA* **103**:10414–10419.
29. Neely, M. N., J. D. Pfeiffer, and M. Caparon. 2002. Streptococcus-zebrafish model of bacterial pathogenesis. *Infect. Immun.* **70**:3904–3914.
30. Nusslein-Volhard, C., and R. Dahm. 2002. Zebrafish: a practical approach. Oxford University Press, New York, NY.
31. Payne, D. J., M. N. Gwynn, D. J. Holmes, and D. L. Pompliano. 2007. Drugs for bad bugs: confronting the challenges of antibacterial discovery. *Nat. Rev. Drug Discov.* **6**:29–40.
32. Pearson, J. P., M. Feldman, B. H. Iglewski, and A. Prince. 2000. *Pseudomonas aeruginosa* cell-to-cell signaling is required for virulence in a model of acute pulmonary infection. *Infect. Immun.* **68**:4331–4334.
33. Peterson, R. T., S. Y. Shaw, T. A. Peterson, D. J. Milan, T. P. Zhong, S. L. Schreiber, C. A. MacRae, and M. C. Fishman. 2004. Chemical suppression of a genetic mutation in a zebrafish model of aortic coarctation. *Nat. Biotechnol.* **22**:595–599.
34. Prajsnar, T. K., V. T. Cunliffe, S. J. Foster, and S. A. Renshaw. 18 August 2008, posting date. A novel vertebrate model of *Staphylococcus aureus* infection reveals phagocyte-dependent resistance of zebrafish to non-host specialized pathogens. *Cell. Microbiol.* doi:10.1111/j.1462-5822.2008.01213x.
35. Pressley, M. E., P. E. Phelan III, P. E. Witten, M. T. Mellon, and C. H. Kim. 2005. Pathogenesis and inflammatory response to *Edwardsiella tarda* infection in the zebrafish. *Dev. Comp. Immunol.* **29**:501–513.
36. Pukatzki, S., R. H. Kessin, and J. J. Mekalanos. 2002. The human pathogen *Pseudomonas aeruginosa* utilizes conserved virulence pathways to infect the social amoeba *Dictyostelium discoideum*. *Proc. Natl. Acad. Sci. USA* **99**:3159–3164.
37. Rahme, L. G., F. M. Ausubel, H. Cao, E. Drenkard, B. C. Goumnerov, G. W. Lau, S. Mahajan-Miklos, J. Plotnikova, M. W. Tan, J. Tsongalis, C. L. Walendziewicz, and R. G. Tompkins. 2000. Plants and animals share functionally common bacterial virulence factors. *Proc. Natl. Acad. Sci. USA* **97**:8815–8821.
38. Rahme, L. G., M. W. Tan, L. Le, S. M. Wong, R. G. Tompkins, S. B. Calderwood, and F. M. Ausubel. 1997. Use of model plant hosts to identify *Pseudomonas aeruginosa* virulence factors. *Proc. Natl. Acad. Sci. USA* **94**:13245–13250.
39. Rawls, J. F., M. A. Mahowald, A. L. Goodman, C. M. Trent, and J. I. Gordon. 2007. *In vivo* imaging and genetic analysis link bacterial motility and symbiosis in the zebrafish gut. *Proc. Natl. Acad. Sci. USA* **104**:7622–7627.
40. Rhodes, J., A. Hagen, K. Hsu, M. Deng, T. X. Liu, A. T. Look, and J. P. Kanki. 2005. Interplay of pu.1 and gata1 determines myelo-erythroid progenitor cell fate in zebrafish. *Dev. Cell* **8**:97–108.
41. Rozen, S., and H. J. Skaletsky. 2000. Primer3 on the WWW for general users and for biologist programmers, p. 365–386. *In* S. Krawetz and S. Misener (ed.), *Bioinformatics methods and protocols: methods in molecular biology*. Humana Press, Totowa, NJ.
42. Rumbaugh, K. P., J. A. Griswold, B. H. Iglewski, and A. N. Hamood. 1999. Contribution of quorum sensing to the virulence of *Pseudomonas aeruginosa* in burn wound infections. *Infect. Immun.* **67**:5854–5862.
43. Schweizer, H. P. 1991. *Escherichia-Pseudomonas* shuttle vectors derived from pUC18/19. *Gene* **97**:109–112.
44. Shestopalov, I. A., S. Sinha, and J. K. Chen. 2007. Light controlled gene silencing in zebrafish embryos. *Nat. Chem. Biol.* **3**:650–651.
45. Smith, E. E., D. G. Buckley, Z. Wu, C. Saenphimmachak, L. R. Hoffman, D. A. D'Argenio, S. I. Miller, B. W. Ramsey, D. P. Speert, S. M. Moskowitz, J. L. Burns, R. Kaul, and M. V. Olson. 2006. Genetic adaptation by *Pseudomonas aeruginosa* to the airways of cystic fibrosis patients. *Proc. Natl. Acad. Sci. USA* **103**:8487–8492.
46. Smith, R. S., M. C. Wolfgang, and S. Lory. 2004. An adenylate cyclase-controlled signaling network regulates *Pseudomonas aeruginosa* virulence in a mouse model of acute pneumonia. *Infect. Immun.* **72**:1677–1684.
47. Stern, H. M., R. D. Murphey, J. L. Shepard, J. F. Amatruda, C. T. Straub, K. L. Pfaff, G. Weber, J. A. Tallarico, R. W. King, and L. I. Zon. 2005. Small molecules that delay S phase suppress a zebrafish *bmyb* mutant. *Nat. Chem. Biol.* **1**:366–370.
48. Tan, M. W., S. Mahajan-Miklos, and F. M. Ausubel. 1999. Killing of *Caenorhabditis elegans* by *Pseudomonas aeruginosa* used to model mammalian bacterial pathogenesis. *Proc. Natl. Acad. Sci. USA* **96**:715–720.
49. Tan, M. W., L. G. Rahme, J. A. Sternberg, R. G. Tompkins, and F. M. Ausubel. 1999. *Pseudomonas aeruginosa* killing of *Caenorhabditis elegans* used to identify *P. aeruginosa* virulence factors. *Proc. Natl. Acad. Sci. USA* **96**:2408–2413.
50. Trede, N. S., D. M. Langenau, D. Traver, A. T. Look, and L. I. Zon. 2004. The use of zebrafish to understand immunity. *Immunity* **20**:367–379.
51. Ulloa, L., and K. J. Tracey. 2005. The 'cytokine profile': a code for sepsis. *Trends Mol. Med.* **11**:56–63.
52. Vance, R. E., A. Rietsch, and J. J. Mekalanos. 2005. Role of the type III secreted exoenzymes S, T, and Y in systemic spread of *Pseudomonas aeruginosa* PAO1 in vivo. *Infect. Immun.* **73**:1706–1713.
53. van der Sar, A. M., R. J. Musters, F. J. van Eeden, B. J. Appelmek, C. M. Vandenbroucke-Grauls, and W. Bitter. 2003. Zebrafish embryos as a model host for the real time analysis of *Salmonella typhimurium* infections. *Cell. Microbiol.* **5**:601–611.
54. Yahr, T. L., and M. C. Wolfgang. 2006. Transcriptional regulation of the *Pseudomonas aeruginosa* type III secretion system. *Mol. Microbiol.* **62**:631–640.